Robust gain scheduling control for wave energy conversion

Ferri, Francesco; Kramer, Morten B.

Published in:
IFAC-PapersOnLine

DOI (link to publication from Publisher):
10.1016/j.ifacol.2020.12.1177

Publication date:
2020

Document Version
Publisher's PDF, also known as Version of record

Available online at www.sciencedirect.com

ScienceDirect

IFAC PapersOnline CONFERENCE PAPER ARCHIVE

IFAC PapersOnLine 53-2 (2020) 12301–12306

Robust Gain Scheduling Control for Wave Energy Conversion

Francesco Ferri * **Morten B. Kramer** *, **

* *Department of the Built Environment, Aalborg University, Aalborg DK (e-mail: ff@build.aau.dk).*

** *Floating Power Plant A/S, Bandholm DK*

Abstract: Enhancing the power performance of wave energy converters is undoubtedly a step required to reduce the cost of energy from this source of renewable energy, thereby making it competitive to other sources of renewable energy. Increasing the power absorption can be achieved by utilizing smart and advanced control algorithms. There are theories for a variety of advanced control algorithms, but few have proved stable and reliable for real applications. An often used, and robust method for practical applications, is to apply a simple gain scheduling controller where the control gains are parameterized in function of the sea state, and not at wave-by-wave level. This paper presents a wave-by-wave adaptive controller, which has proven a robust method that can increase the power absorption performance. The use of the wave by wave adaptive controller is achieved by the identification of the instantaneous fundamental frequency in real time. One numerical procedure to achieve this frequency is using non-linear Kalman filters. But the pitfall of these non-linear filters is their sensitivity to the parameter tuning, which decreases practical usability, reliability and robustness. This paper focuses on two complementary topics. The first topic will tackle the implementation of a reliable filter for the identification of the instantaneous fundamental frequency using a particle filter. The second topic will demonstrate the implementation of the wave-by-wave gain scheduling controller. The case study is a scaled absorber of the Floating Power Plant wave and wind energy converter.

Keywords: Particle Filter, Fundamental Frequency, Wave Energy Control

1. INTRODUCTION

In the attempt to shift the energy production from fossil fuels to more sustainable choices, a growing number of renewable energy resources have been used or theorized. While wind, solar, hydro, geothermal, and biomass are established technologies, other sectors are not mature yet; nevertheless, their development is fundamental to balancing the future energy mix. Within those untapped resources, ocean waves retain a huge energy potential, but ocean waves converters, better known as Wave Energy Converters (WEC), are still not ready from a cost perspective. Several machines have proven the feasibility of the concepts, regardless of the rough environment, but not the economical viability of the project.

Optimizing the generator load in order to increase the energy conversion efficiency is the most straightforward way to decrease the cost of energy associated with WECs. A variety of control algorithms have been adapted to fit the requirements from the wave energy sector, for example:

- fixed gain feedback controller (Kramer et al. (2011))
- predictive controller (Coe et al. (2016); Beatty et al. (2017))
- other controller type (Davidson et al. (2017); Fusco and Ringwood (2012); Nguyen and Tona (2017))

This work will only focus on the so called passive feedback controller. The rationale behind this choice is the following: "When we try to have an impedance matching controller, the reverse flow of energy from the grid to the wave is often times equal or even larger than the absorbed energy: the global result are slightly better or even worse than a simple damping control", (see Ferri et al. (2016)).

A passive feedback controller, with the proportional (K_P) gain scheduled in function of the sea state, has been extensively used due to its implementation simplicity. A sea state is considered to be statistically constant over a period of roughly 15-30 minutes; therefore, the controller gains can be changed on the same time scale. But since the optimal controller gains depend on the wave frequency and since a sea state is composed of multiple frequencies, it might be beneficial to adapt the gains for each frequency component, (Fusco and Ringwood (2012); Nguyen and Tona (2017)). A critical step in those approaches is the identification of the instantaneous fundamental frequency of the excitation load. The same problem is encountered in several other fields, such as power transmission or music, and typically the Hilbert transform is adopted. Nevertheless, since the Hilbert transform is a non-linear transformation, its real-time implementation can be problematic.

The majority of the studies, available in the literature, that use a real-time Hilbert transform adopt different non-linear extensions of the Kalman filter. The non-linear version of the Kalman filter is powerful, but also retains some limitation; the most critical limitation being the parameter tuning. There is no univocal method to tune

10.1016/j.ifacol.2020.12.1177

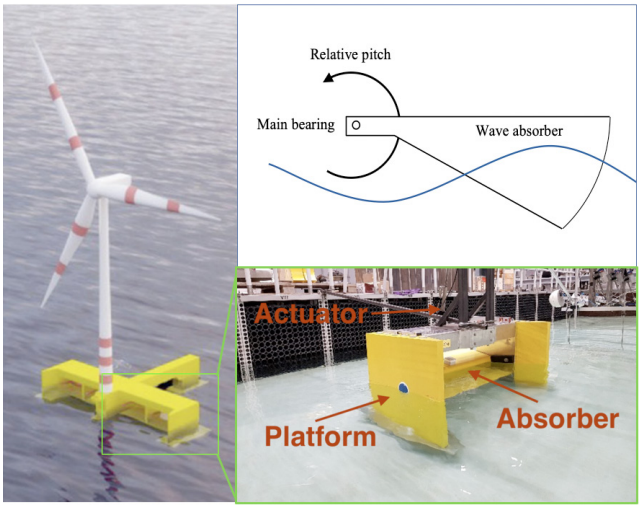

Fig. 1. FPP machine. Left Side: P80 full machine rendering. Top Right Side: working principle of the absorber. Bottom Right Side: 1:30 scaled physical model of the wave absober section of the P80.

the parameters of a non-linear Kalman filter, but the filter stability depends on this step and, albeit being crucial, often no or little remarks can be found on this topic. In order to avoid this uncertain step, this work makes use of a different filter type, namely the Particle filter (PF).

Once the instantaneous wave frequency has been identified, it is possible to adapt the controller gain(s) to the actual condition, implementing a wave-by-wave adaptive controller or gain scheduling controller (GSC), similar to the one proposed in Fusco and Ringwood (2012) and Nguyen and Tona (2017).

The results presented in this work are all based on experimental data. Therefore the non-linear filter and the GSC were implemented in real-time on a scaled WEC model. Due to space constraint, it has not been possible to also include the numerical results in this work.

The experimental device is a subsection of the Floating Power Plant (FPP) machine, reported in Fig. 1. The FPP is a combined wind-wave energy converter, but in this campaign only one half of the wave converter portion is used. The machine scaled is 1:30 and it consists of a platform, an absorber, and a power take-off (PTO) system. The absorber is hinged and can only move in a single degree of freedom (pitch) relative to the platform. The PTO is modeled using a linear electrical actuator, which is controlled using real-time operating system similar to the one presented in Ringwood et al. (2017).

In the reported tests the platform was held fixed so the only active degree of freedom was the pitch of the absorber. A numerical study considering the complete multidof system with 6 dof motions of the platform and individual pitching absorbers relative to the platorm, showed that an ideal GSC has the potential to improve the power absorption up to 45% in some sea states. However, as this is yet to be proven in practical experimental tests focus in the following is on the measurements on the single degree of freedom device.

For further information, see Rippol and Thomas (2018).

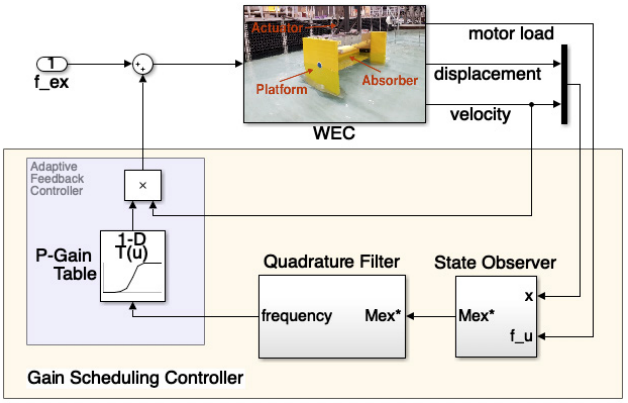

Fig. 2. GSC framework: "WEC" represents the actual machine, "State Observer" is the excitation load observe, "Quadrature Filter" is the non-linear instantaneous frequency observer for the excitation load and "Adaptive Feedback Controller" is the adaptive control estimator.

The experimental campaign was carried out at the Department the Built Environment, Aalborg University (AAU). The basin is equipped with long-stroke segmented piston wave-maker for accurate short-crested (3-dimensional) random wave generation with active absorption. Further information is given in Tetu et al. (2017).

To summarize, the main objectives of this article are as follows:

- to verify the usability of a particle filter to replace a non-linear Kalman filter in a physical model and
- to implement and compare the GSC with a sea state static gain feedback controller in the same physical model.

The methods are presented in Sec. 2 along with the description of the material used for the physical implementation, while the results and their discussion are summarized in Sec. 3. Finally, the conclusions of the work are given in Sec. 4.

2. METHODS

This section introduces the main methods used throughout the study. For simplicity the main controller architecture is shown in Fig. 2. The GSC architecture can be divided in four building blocks:

State Observer is the stage where the load exciting the system is estimated, see Sec 2.1

Quadrature Filter is the stage where the excitation load frequency and amplitude are assessed, see Sec 2.2

Adaptive Feedback Controller is the block where the control signal is estimated based on the actual state of the system and based on the excitation load frequency and amplitude, see Sec. 2.3.

2.1 Excitation Load Observer

In order to identify the frequency and amplitude of the wave excitation load, it is necessary to obtain the excitation load itself. Since it is not possible to directly measure the excitation load, a soft-sensing technique based

on linear Kalman filter is adopted, as introduced in several studies, see Ferri et al. (2015) and Hals et al. (2011). The Kalman filter is built around the linear numerical model of the WEC; this can be obtained using experimental data or numerical models. In the latter case, a linear diffraction-radiation numerical model is commonly used. The state space formulation of the WEC follows the form presented in Yu and Falnes (1995). The system state is augmented then with the excitation force state. For this application a simple integrator for the excitation model was sufficient, but other alternatives are possible, e.g. single or multiple oscillators, auto regressive models, etc. The measured velocity and displacement were used in the Kalman filter update stage.

2.2 Quadrature Filter

Once the excitation load has been estimated, it is possible to extract its baseband signal, which is the fundamental harmonic of the signal. As mentioned in the introduction, the Hilbert transform or quadrature filter will be used to estimate the fundamental frequency of the signal. For a narrow-banded signal ($s(t)$), its analytic signal ($s^+(t)$) is defined as:

$$s^+(t) = s(t) + jH[s(t)] \tag{1}$$

where j is the complex operator and $H[]$ represents the Hilbert operator. Using the polar representation of the analytic signal, it is possible to extract the instantaneous amplitude ($a(t)$) and frequency ($w(t)$).

$$s^+(t) = a(t)e^{j\phi(t)} \tag{2}$$

$$w(t) = \frac{d\phi}{dt} \tag{3}$$

ϕ is the phase of the analytical signal ($s^+(t)$). The state space representation of the Hilbert transform described in Fusco and Ringwood (2010) will be used, which is:

$$x_k = A(x)x_{k-1} + \upsilon_k \tag{4}$$

$$\tag{5}$$

where:

$$A = \begin{bmatrix} \cos(x_3/f_s) & \sin(x_3/f_s) & 0 \\ -\sin(x_3/f_s) & \cos(x_3/f_s) & 0 \\ 0 & 0 & 1 \end{bmatrix} \tag{6}$$

Here, f_s represents the sample frequency in Hz, k is the discrete time index, υ is the vector of random disturbances and $x_k = [\phi, \phi^*, \omega]$ is the state vector. ω is the instantaneous fundamental frequency and the excitation load amplitude $|M_{ex}|$ is defined as $\sqrt{\phi^2 + \phi^{*2}}$.

Unscented Kalman Filter This section provides a short description of the unscented Kalman filter (UKF), but the reader can find further details in Lefebvre et al. (2004). Contrary to the extended Kalman filter, where the process and measurement functions are linearized using a first order Taylor expansion around the updated state estimated, the UKF linearizes the process and measurement functions by statistical linear regression of the sampling points. These sampling points are chosen such that their mean and covariance matrix equals the estimated state and its covariance. The linear regression minimizes the error in the least square sense, between the linearized and non-linearized function at the sampling points. This approach has been used in Nguyen et al. (2017), as a solution to the divergence phenomena associated with Extended Kalman filter as presented in Fusco and Ringwood (2012). Nevertheless, as shown in the result section, the UKF performance is also sensitive to the parameter definitions, and for some parameters there is no straight forward identification procedure.

Particle Filter Particle filter (PF) is a sequential Monte Carlo method that does not estimate the state directly but from the posterior probability ($p(x_k|y_k)$) as:

$$p(x_k|y_k) = \sum_{i=1}^{N} w_k^i \delta(x_k - x_k^i) \tag{7}$$

Here y_k is the set of accumulated measurement up to time k, N represents the number of particles, w_k^i is the particle importance weight, and x_k^i is the particle state. At each time k the particles are defined as:

$$P(k) = \langle (x_k^i, w_k^i) | i \in 1, ..., N \rangle \tag{8}$$

The main PF algorithm consists of Sampling, Importance weight, and Resampling. In the Sampling phase the proposal distribution ($q(x_k^i|x_{k-1}^i, y_k)$) is used to generate the samples. In this study the posterior function $p(x_k|y_k)$ is used:

$$q(x_k^i|x_{k-1}^i, y_k) = p(x_k^i|x_{k-1}^i, y_k) \tag{9}$$

Since this is a critical design choice, the reader can find further information in Arulampalam et al. (2002). During the Importance weight stage, the weights of the particle are updated based on the prior state and measurements. Finally, in the Resample phase the particles are resampled based on the weight in order to keep only the meaningful particles. The key parameter for the PF is N, which limited the utilization of this method until recent years due to the computational cost. PF are widely used in robotic/positioning applications (Gustafsson (2010)) and for non-linear system identification (Schön (2015)).

2.3 Adaptive Feedback Controller

The main controller used in this study is a simple feedback controller, where the load exerted by the generator on the absorber is proportional to the actual state of the system. As presented in Hansen and Kramer (2011) the control load can be proportional to the full state of the system or just to a part of it. If the displacement and/or the acceleration of the system are used, the controller is capable of extending the bandwidth of the system, similar to the impedance matching controller introduced in Falnes (2002). Nevertheless, the use of a reactive/active controller requires a reverse flow of energy, from the grid to the absorber, which becomes promptly inconvenient or only marginally convenient if the conversion chain efficiency has to be considered.

Based on numerical results and based on the chosen transformation efficiency of 70%, it has been decided to

only use a passive controller, proportional to the velocity of the absorber, defined as:

$$f_u(k) = K_P(k)v(k) \tag{10}$$

Here, f_u represents the power take-off load, K_P is the controller gain, and v is the absorber velocity.

K_P is selected from a precomputed look-up table in function of the fundamental frequency at time k. The look-up table is based on experimental tests in regular waves, which are not reported here due to space limitation. The K_P search is configured to not extrapolate value outside the given frequency range, and to use the closest frequency range limit instead.

3. RESULT AND DISCUSSION

This section presents and provides discussion of the main results of the PF and in general of the GSC; the section follows closely the structure of the previous one.

A total of six irregular sea states were used to estimate the power performance of the system: each condition contains at least 1000 waves to ensure statistical convergence. The conditions are reported in Tab. 1 in function of the significant wave height H_{m0} and the peak period T_p. The prefix IR is an abbreviation of irregular, used to distinguish between regular and irregular wave conditions. The waves are generated using a white noise method and the parameterized JONSWAP ($\gamma = 1.5$) has been used. For each sea state the wave generation signal is recorded and repeated to ensure a direct comparison between different controller setup.

Table 1. Sea State condition used in the test campaign

	IR1	IR2	IR3	IR4	IR5	IR7
H_{m0} (m)	0.035	0.035	0.035	0.035	0.035	0.075
T_p (s)	1.1	1.5	1.7	2.0	2.5	2.0

3.1 Excitation Load Observer

In order to assess the quality of estimated excitation load, it is important to measure the excitation load in first place. This is possible by locking the absorber at the equilibrium position and measuring the load at the connection point of the motor. Since the whole GSC is based on the availability of a reliable excitation load measurement, the validation of this step is of paramount importance.

From Fig. 3 it is possible to conclude that the linear Kalman observer is well suited to estimate the excitation load from the system state for this particular machine. The goodness of fit between the two signal in the figure is 0.9957, and no condition with a goodness of fit below 0.985 was observed. The goodness of fit has been estimated using the normalised mean square error. The zoomed view of Fig. 3 (top-right corner), highlights the noise introduced in the estimated signal, in particular a 50Hz noise component was present. Although it is possible to introduce a smoothing effect in the Kalman observer design, this might result in a phase shift between the two signals, which in turn deteriorates the overall estimation accuracy (goodness of fit 0.95). It is possible to reduce the noise, without phase

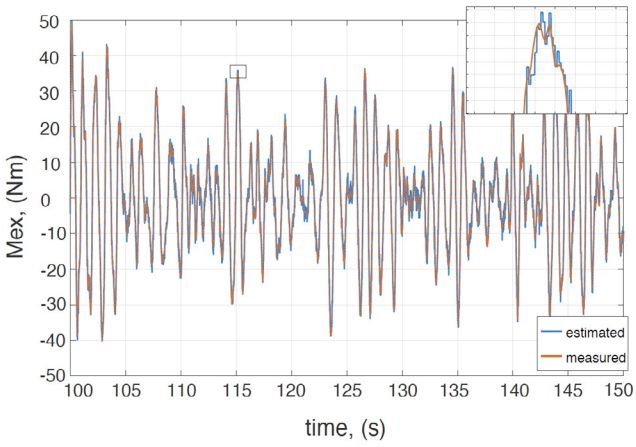

Fig. 3. Deterministic comparison of the observed (blue line) and measured (red line) excitation loads (Mex) for the sea state IR1. The top right box is a zoomed section of the signal to highlight the signal noise.

deterioration, by using one or multiple oscillators for the excitation load model as shown in Fusco and Ringwood (2010). However, there was no evident benefit for this particular application, and the controller was able to cope with the level of noise introduced in the estimator.

3.2 Quadrature Filter

Once the accuracy of the excitation load observer is assessed, it is possible to analyze the performance of the two implementation of the quadrature filters. Fig. 4 is particularly important because it highlights the main motivation of this study. Three different cases can be identified:

Top Plot both PF and UKF are able to correctly demodulate the excitation load signal.

Middle Plot the PF deviates from the correct solution, but it is able to reduce the error in about 40 seconds

Bottom Plot the UKF diverges from the correct solution and does not recover within the whole test.

As will be shown in the following figures, the UKF performs better than the PF: for example reduced time to converge and better noise rejection. But in some of the tested conditions, the UKF became unstable. This instability was triggered randomly and at least once for each of the tested sea states. It was not possible to identify a clear cause for the instability to happen. A sea state with an unstable UKF, would produce 10-20% less energy if compared with a fixed gain controller, due to the non-optimality of the controller gain.

All the filters, linear KF, PF, and UKF, were designed using a numerical model of the WEC. The model was estimated from experimental data in order to reduce the inconsistency between numerical and experimental results. Due to the difficulties to design a stable UKF, global optimization methods have been tested also. Although it was possible to identify a stable UKF for each sea state, it was not possible to obtain a stable design across the different conditions. Since the implementation of an adaptive UKF would have added more complexity to the system, it was decided to only use the best UKF found.

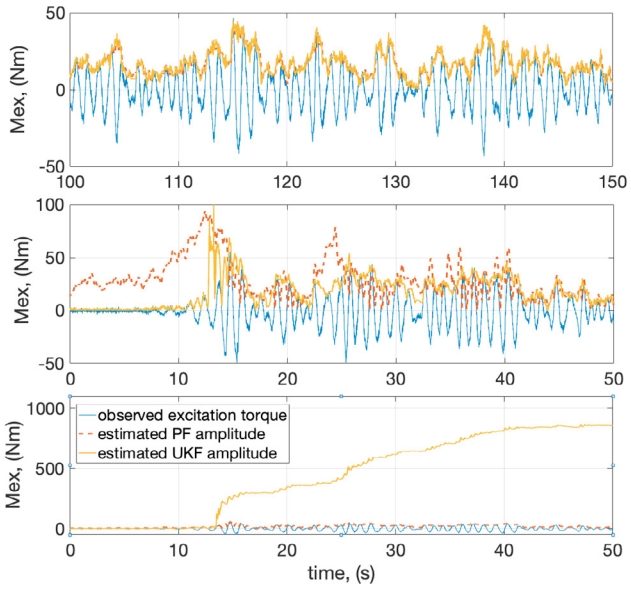

Fig. 4. Comparison of the UKF (yellow line) and PF (red line) observed excitation load amplitudes for the sea state IR1. The measured excitation load (blue line) is used for reference. (Top) fully developed sea state, (Mid) highlights of the initial condition divergence for the PF, and (Bottom) highlights of the initial condition divergence for the UKF.

The uncertainty in the parameter definition for the UKF is the main limitation for its usage in the author point of view, and little emphasis is given to this problem in available literature.

On the other hand, the PF produces similar results, with comparable implementation effort and ease of tuning: the major tuning parameter being the number of particle. The process noise was estimated empirically. In order to estimate its influence on the filter performance, a sensitivity study was carried out, which resulted in a negligible filter performance degradation.

Fig. 5 gives a visual indication of the effect of the number of particles. The plot represents the timeseries of the estimated instantaneous fundamental frequency, for two PFs and the UKF. The vertical black dotted line represents the end of the wave ramp-up phase. The black line represents a PF with 20 particles, while the blue line a PF with 2000. There is a great reduction of the ramp up time, when more particles are used, but the tracking performance is not deteriorated after the transient condition. Fig. 5 also shows that the UKF (red line) results in a quicker response to the transient or lower settling time. The filter reaches a steady condition in 1-2s while the PF requires at least 10-20s. Once more, after the transient condition the filter results are comparable.

During the experimental campaign the PF with 2000 particles was used, because 20 particles resulted in a longer waiting time and 5000 particles did not increase the quality of the results. Since a hard real-time operating system was adopted, it is important to ensure that the cpu is never overloaded: in the worst condition the average computational time was 1/100 the sample time of 1ms.

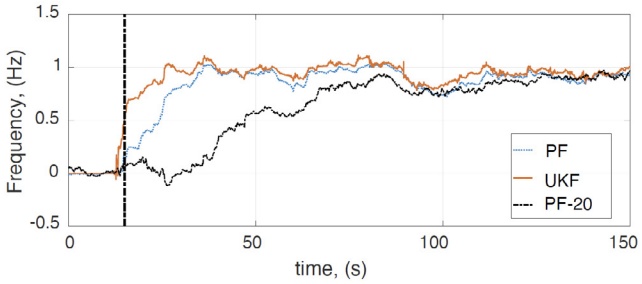

Fig. 5. Observed frequency comparison between UKF (red line), PF (blue line), and under-sampled PF (black line). The ending of the wave ramp-up time is marked with a vertical dotted line.

3.3 Gain Scheduling Controller

The results of the GSC are compared with the max absorbed average power using static K_P values. The max average power is obtained by running each sea state six times, each time with a different value of K_P.

The optimal K_P range lies in the range 100-140 Nm/(rad/s) for the tested condition. It is important to notice though, that changing any of the sea state parameters (H_{m0}, Tp, γ, spectral distribution, etc...) will require the optimal K_P identification procedure to be re-run. This is probably the main limiting factor of the static gain methodology.

Tab. 2 summarises the main comparison between the controller optimized for every sea state and the adaptive one. The table reports the average power performance for each sea state, for the two controller, and in the bottom row the difference in % is given. On the average of the 7 sea states, 2.5% improvement is achieved, with a low value of -6% and a max value of 4%. It is important to notice that the positive results are obtained in the energetic sea state while the negative results are obtained in the less energetic sea state. Therefore using a weighted average will improve the result outlook.

Table 2. Average power production in function of the sea state and control type

Controller	IR1	IR2	IR3	IR4	IR5	IR7
Static	0.613	0.811	0.829	0.853	0.719	3.839
Adaptive	0.574	0.817	0.86	0.863	0.74	3.99
Diff.(%)	-6.3	0.74	3.74	1.17	2.92	3.93

4. CONCLUSION

The work presented in this study aims at increasing the power production of wave energy converters from a controller prospective, covering two main objective:

- robust/reliable implementation of a real-time quadrature filter (Hilbert transform) to identify the baseband frequency of the excitation load using a Particle Filter.
- implementation of the gain scheduling controller, where the instantaneous baseband frequency is used to adapt the K_P of the outer feedback controller.

It is important to highlight that the overall frame is not new in the wave energy sector (cf. Fusco and Ringwood (2012) and Nguyen et al. (2017)). Firstly the system has

been validated in a real-time implementation, with all the embedded difficulties, and secondly the usage of Particle filter for non-linear observer has not been used before for similar applications to the author's knowledge.

The Particle filter has been compared with the Unscented Kalman filter through the article.

As shown in the results, the Particle filter returns similar results if compared with a Unscented Kalman filter, while providing two main advantages:

(1) simpler tuning procedure
(2) higher filter stability in function of the tuned parameters

Furthermore, within this study, the performance of the GSC has been compared with a sea state optimized static gain controller. Although the benefits of the GSC might seem minimal (5%), they have a direct positive effect on the cost of energy for the given machine. Assuming that no additional cost will be introduced due to the GSC, the economical benefit are directly related to the increased power production. The costs for the controller design and implementation and the operational cost of the controller are marginal and do no effect on the overall cost.

The results of this study might be used as a starting point for a more detailed economical analysis and for the implementation into the full FPP machine.

ACKNOLEDGMENTS

The work reported here was carried out in the project "Digital Hydraulic Power Take Off for Wave Energy" which is funded through the ForskEL programme by Energinet and this funding is gratefully acknowledged.

REFERENCES

Arulampalam, M.S., Maskell, S., Gordon, N., and Clapp, T. (2002). A tutorial on particle filters for online nonlinear/non-gaussian bayesian tracking. *IEEE Transactions on signal processing*, 50(2), 174–188.

Beatty, S., Ferri, F., Bocking, B., Kofoed, J., and Buckham, B. (2017). Power take-off simulation for scale model testing of wave energy converters. *Energies*, 10(7), 973.

Coe, R.G., Bacelli, G., and Wilson, D.G. (2016). Advanced wec dynamics and controls. Technical report, Sandia National Lab.(SNL-NM), Albuquerque, NM (United States).

Davidson, J., Genest, R., and Ringwood, J.V. (2017). Adaptive control of a wave energy converter simulated in a numerical wave tank. In *Proceedings of the 12th European Wave and Tidal Energy Conference (EWTEC 2017), Cork*.

Falnes, J. (2002). *Ocean waves and oscillating systems: linear interactions including wave-energy extraction*. Cambridge university press.

Ferri, F., Ambühl, S., and Kofoed, J.P. (2015). Influence of the excitation force estimator methodology within a predictive controller framework on the overall cost of energy minimisation of a wave energy converter. *International Conference on Computational Methods in Marine Engineering*.

Ferri, F., Tetu, A., and Hals, J. (2016). Practical performances of mpc for wave energy converters. In *International Conference on Renewable Energies Offshore*, 453–462. CRC Press.

Fusco, F. and Ringwood, J.V. (2010). Short-term wave forecasting for real-time control of wave energy converters. *IEEE Transactions on sustainable energy*, 1(2), 99–106.

Fusco, F. and Ringwood, J.V. (2012). A simple and effective real-time controller for wave energy converters. *IEEE Transactions on sustainable energy*, 4(1), 21–30.

Gustafsson, F. (2010). Particle filter theory and practice with positioning applications. *IEEE Aerospace and Electronic Systems Magazine*, 25(7), 53–82.

Hals, J., Falnes, J., and Moan, T. (2011). Constrained optimal control of a heaving buoy wave-energy converter. *Journal of Offshore Mechanics and Arctic Engineering*, 133(1), 011401.

Hansen, R.H. and Kramer, M.M. (2011). Modelling and control of the wavestar prototype. In *The 9th European Wave and Tidal Energy Conference: EWTEC 2011*. University of Southampton.

Kramer, M., Marquis, L., Frigaard, P., et al. (2011). Performance evaluation of the wavestar prototype. In *Proceedings of the 9th European Wave and Tidal Energy Conference, Southampton, UK*, 5–9. Citeseer.

Lefebvre, T., Bruyninckx, H., and De Schutter, J. (2004). Kalman filters for non-linear systems: a comparison of performance. *International journal of Control*, 77(7), 639–653.

Nguyen, H.N. and Tona, P. (2017). Continuously Adaptive PI Control of Wave Energy Converters under Irregular Sea-State Conditions. In *12th European Wave and Tidal Energy Conference 2017*. Cork, Ireland.

Nguyen, H.N., Tona, P., and Sabiron, G. (2017). Dominant wave frequency and amplitude estimation for adaptive control of wave energy converters. In *OCEANS 2017-Aberdeen*, 1–6. IEEE.

Ringwood, J., Ferri, F., Ruehl, K., Yu, Y.H., Coe, R., Bacelli, G., Weber, J., and Kramer, M.M. (2017). A competition for wec control systems. In *12th European Wave and Tidal Energy Conference*. Technical Committee of the European Wave and Tidal Energy Conference.

Rippol, T. and Thomas, S. (2018). *FPP Marinet2 Tests at Oceanide*. FPP. URL `http://www.marinet2.eu/wp-content/uploads/2019/01/D40.1.R.FPP_.PlatformModelTests.pdf`.

Schön, T.B. (2015). Nonlinear system identification using particle filters. *Encyclopedia of Systems and Control*, 882–890.

Tetu, A., Andersen, T.L., and Kofoed, J.P. (2017). *Ocean and Coastal Engineering Laboratory*. AAU. URL `"https://www.en.build.aau.dk/laboratories/ocean-and-coastal-engineering/#448389"`.

Yu, Z. and Falnes, J. (1995). State-space modelling of a vertical cylinder in heave. *Applied Ocean Research*, 17(5), 265–275.